

## Intraband inversion due to ultrashort carrier lifetimes in proton-bombarded InP

R. A. Höpfel, Ch. Teissl, and K. F. Lamprecht

*Institut für Experimentalphysik, Universität Innsbruck, A-6020 Innsbruck, Austria*

L. Rota

*Clarendon Laboratory, University of Oxford, Parks Road, Oxford OX1 3PU, United Kingdom*

(Received 14 August 1995; revised manuscript received 18 September 1995)

We report the evidence of occupation inversion in time average within the continuous band structure of the semiconductor InP. Ultrafast carrier trapping and recombination ( $\tau \approx 1 \times 10^{-13}$  s) as a consequence of proton bombardment prevents the thermalization of optically excited electron-hole pairs ( $n \sim 3 \times 10^{16}$  cm $^{-3}$ ). Beyond previous experimental observations of inverted time-averaged luminescence spectra, we present experimental data at lower carrier concentrations, which are in quantitative agreement with ensemble Monte Carlo simulations. Inverted electron and hole energy distributions are determined quantitatively. We propose the application for a solid-state free-electron laser.

The temporal evolution of the energy distribution of photoexcited carriers in semiconductors has been a major research topic over the past decade.<sup>1</sup> The spectral width of ultrashort laser pulses, the semiconductor band structure, and the ultrafast dephasing<sup>2</sup> determine the initial nonequilibrium carrier distribution. The fast transition into a hot Fermi-Dirac distribution—known as “thermalization”—occurs mainly through carrier-carrier collisions, supported by phonon scattering. Quantitative knowledge of the thermalization process is important for a full understanding of the ultrafast relaxation processes in solids. In addition, the knowledge of thermalization is essential for realizing stimulated emission *within* one band of a semiconductor,<sup>3</sup> where population inversion must be maintained against the thermalization process. The time scale of the thermalization process is sensitive to the carrier concentration and the energy of the injected carriers. Experiments have been performed in various ranges of these two parameters,<sup>4–12</sup> giving a consistent quantitative picture of the thermalization process in semiconductors, such as GaAs and InP. Strongly nonthermal distributions exist only for less than 100 fs at carrier densities around  $10^{17}$  cm $^{-3}$ .<sup>9,11,13</sup> In the range of  $10^{16}$  cm $^{-3}$ , the thermalization rate is comparable to the emission rate of optical phonons ( $\sim \frac{1}{180}$  fs $^{-1}$ ),<sup>11,12</sup> for carrier densities below  $10^{14}$  cm $^{-3}$  the thermalization time can reach up to 50 ps.<sup>10</sup>

In this paper, we report a striking consequence of the finite thermalization time. In semiconductors with extremely short carrier lifetimes, limited by trapping and recombination, the lifetime of photoexcited carriers in the continuous bands can be comparable or even shorter than the thermalization time. In this case, the time averaged carrier distributions will be dominated by the initial injection energy and can deviate substantially from thermal distributions.<sup>14,15</sup> Although we have previously reported on very hot, even inverted luminescence spectra,<sup>15</sup> clear proof of inverted *carrier distributions*, however, has not been given up until now. Here, we will give the experimental and theoretical evidence that—at low enough carrier densities—such a scenario indeed leads to *strongly inverted carrier distributions, time averaged over the full lifetime of the injected carriers.*

Short carrier lifetimes in semiconductors are the consequence of high concentrations of defects,<sup>16,17</sup> which act as traps and recombination centers for photoexcited electrons and holes. For our experiments, we use the III-V-semiconductor InP. The (100) semi-insulating samples ( $\rho \approx 10^7$   $\Omega$  cm) are irradiated with protons of 200 keV; producing a broad damage profile with a maximum of lattice vacancies at a distance of 1.5  $\mu$ m from the surface. The ion doses range from  $1 \times 10^{12}$  up to  $1 \times 10^{16}$  cm $^{-2}$ . The crystallinity, also for the highest damage doses, has been verified by spectral photoconductivity measurements, which show no significant change of the band-gap energy.

The carrier lifetimes in the H<sup>+</sup> irradiated InP crystals have been measured by time-resolved luminescence, using the population correlation method.<sup>15</sup> All experiments are performed at room temperature. The carrier lifetimes have been obtained from the spontaneous luminescence intensity  $I(\hbar\omega, t)$ , given by the bimolecular radiative recombination law,<sup>19</sup> as a function of the electron and hole distributions  $f_e(\mathbf{k}, t)$  and  $f_h(\mathbf{k}, t)$ ,

$$I(\hbar\omega, t) \propto |M_{cv}|^2 \omega^2 D(\hbar\omega) f_e(\mathbf{k}, t) \cdot f_h(\mathbf{k}, t), \quad (1)$$

with the matrix element  $M_{cv}$  for the optical transition and the joint density of states  $D(\hbar\omega)$ . The quantitative results of the lifetime of the photoexcited electron-hole pairs have been reported in Ref. 15: The lifetimes decrease from  $> 100$  ps at an ion dose of  $1 \times 10^{12}$  cm $^{-2}$  down to 95 fs at an ion dose of  $1 \times 10^{16}$  cm $^{-2}$ . The lifetimes have been measured  $\sim 100$  meV above the band gap of InP (due to the sensitivity of the GaAs photomultiplier). Since this measures only the high-energy part of the distribution, an eventual influence of the carrier relaxation might have been involved. We have reproduced, however, the values of Ref. 15 (down to lifetimes of 1 ps) by time-resolved luminescence, using the well-known technique of up-conversion<sup>18</sup> near the band gap.

In the following, we describe the time-integrated luminescence spectra from the sample with a 95-fs carrier lifetime *at low injection densities* ( $10^{16}$ – $10^{17}$  cm $^{-3}$ ), *where the thermalization process is known to be in the 100-fs range.*<sup>11</sup> For

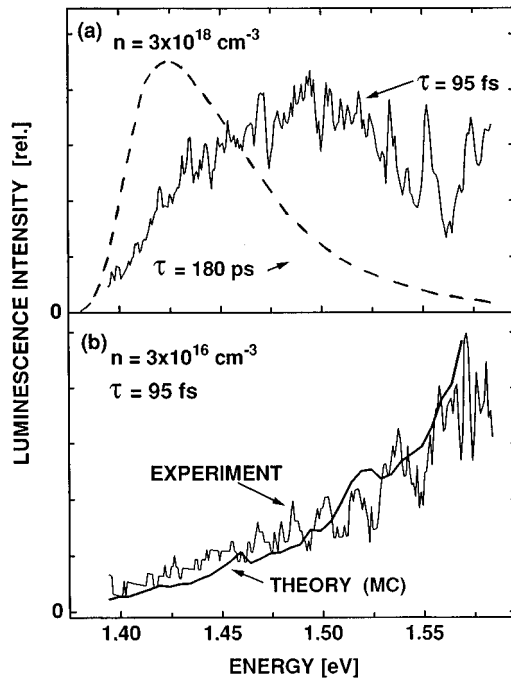


FIG. 1. (a) Spectral band-to-band luminescence (correlation signal) for a sample with a low proton-bombardment dose ( $\tau=180$  ps, dashed curve), and for a high proton-bombardment dose ( $\tau=95$  fs), using high excitation ( $n\sim 3\times 10^{18}$  cm $^{-3}$ ).  $T=300$  K. (b) Low excitation ( $n\sim 3\times 10^{16}$  cm $^{-3}$ ): Experimental luminescence spectra and results of theoretical Monte Carlo simulations.

these experiments, a mode-locked Ti:sapphire laser is used with low excitation densities ( $n\sim 3\times 10^{16}$  cm $^{-3}$ ). Pulse durations are 120 fs, the excitation center wavelength is 730 nm (1.70 eV). The time-integrated luminescence spectra are obtained from the correlation signal of two excitation pulses<sup>15</sup> at relative delay  $\Delta t=0$ . Contributions to the signal, which are linear with excitation power, such as band-impurity luminescence, spontaneous Raman signals, and other light scattering from the surface are excluded, so that only band-to-band luminescence (product of electron and hole distribution) is measured.<sup>15</sup> A low-pass filter is used to cut off the laser stray light above 1.58 eV.

Figure 1(a) shows the luminescence spectra for the sample with a lifetime of 180 ps (dashed line). The maximum of the luminescence intensity is close to the band gap, with an exponential decrease to higher energies, and as expected for a thermalized carrier distribution, cooled down to lattice temperature for almost the complete lifetime of the photoexcited carriers. The luminescence spectra are drastically different for the proton-bombarded sample with a carrier lifetime of 95 fs (full line). The spectrum in Fig. 1(a) taken at high injection density ( $3\times 10^{18}$  cm $^{-3}$ ) is broad, with a maximum around 1.50 eV.

The spectrum in Fig. 1(b), obtained with a much lower excitation density ( $3\times 10^{16}$  electron-hole pairs per cm $^3$ ) shows the most interesting behavior: The luminescence spectrum is *strongly inverted with a monotonous increase of the emission intensity from 1.40 eV up to 1.58 eV*. The data are already spectrally corrected, taking into account the spectral characteristics of the GaAs photomultiplier, the 1.58-eV low-

pass filter, and the monochromator. The spectrally narrow structures in the spectra are only due to noise. Note that the “inversion” of the spectra is much stronger than in Ref. 15, where the photoexcited carrier density was considerably higher ( $\sim 1\times 10^{18}$  cm $^{-3}$ ).

According to Eq. (1), the strongly inverted luminescence spectrum indicates that the ultrashort carrier lifetime time ( $\tau=95$  fs) leads to nonthermal distributions for the main part of the carrier lifetime. For the quantitative interpretation of the luminescence spectra, we compare the experiments with Monte Carlo (MC) simulations, which take into account the complex valence band. We have performed a four-band ensemble MC simulation, including conduction band, heavy, light, and split-off hole bands. LO phonons and the corresponding hot phonon population are considered, as well as interband and intraband hole scattering by TO phonons. Degeneracy effects are included and carrier-carrier scattering is accounted for within a self-consistent static screening approximation, as in Ref. 9. The carrier trapping and nonradiative recombination has been included within a simple model. Taking into account the  $k$  dependence of the trap states and recombination centers (maximum of the wave functions near  $k=0$ ),<sup>16</sup> as well as the fact that the trapping is more likely to occur through phonon emission and carrier-carrier scattering, we used a simple exponential recombination rate peaked at the minimum of each band, with  $1/\tau = \alpha \exp(-k^2/K^2)$ , where  $k$  is the free-carrier wave vector.  $K$  is a constant determined from the experimentally measured recombination heating that will be described later in this paper. The constant  $\alpha$  is determined by the experimentally measured recombination lifetime.

The luminescence spectrum obtained in the MC simulations is shown in Fig. 1(b): The luminescence spectrum is inverted, the relative shape of the spectra agrees well with the experiment, the absolute values of the intensities are not compared. In Figs. 2(a) and 2(b), we show the time integrated distribution functions for electrons and holes corresponding to the luminescence spectrum shown in Fig. 1(b). The electron distribution function shows a well defined inversion over the entire energy range that corresponds to the luminescence spectra. For the holes, the situation is more complicated, both light and split-off holes show mainly an inverted distribution, and the heavy-hole distribution presents a maximum at the top of the band. This is due to the fact that the heavy holes are excited exactly at the threshold for phonon emission and so we can see the phonon replica that is generated at zero energy.

The initial carrier distributions, due to the laser excitation at 1.70 eV, are obviously not thermalized for the main part of the carrier lifetime, for the low carrier concentration of  $3\times 10^{16}$  cm $^{-3}$ . In comparison, the time-resolved luminescence data in Ref. 9 showed no inversion within the time resolution of 100 fs at slightly higher carrier densities of  $1.7\times 10^{17}$  cm $^{-3}$ . The lower carrier concentration in our experiments obviously reduces the electron-electron scattering. The inversion in our experiments, however, is much stronger than expected from this reduction alone. In order to clear the role of the ultrafast trapping and recombination on the intraband relaxation processes, we performed the following additional experiments.

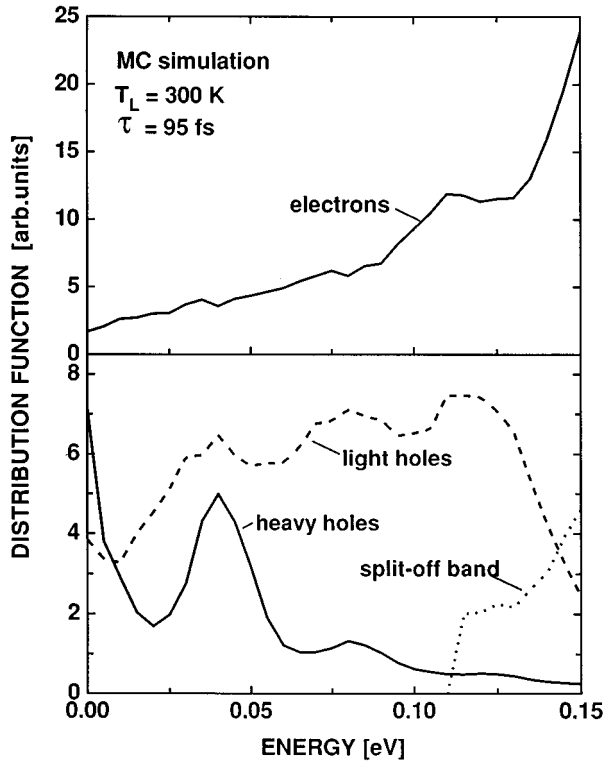


FIG. 2. Carrier distributions as obtained from ensemble Monte Carlo simulations for electrons in the conduction band (upper figure) and holes in the light-hole, heavy-hole, and split-off valence band (lower figure).

Using luminescence up conversion,<sup>18</sup> we studied experimentally the relaxation of the carrier distribution (="cooling curves") for two samples with different proton-bombardment doses, resulting in lifetimes of 180 and 1.5 ps. The time-resolved spectra can be described by effective carrier temperatures, thermalization in these experiments (excitation density  $n \sim 1 \times 10^{18} \text{ cm}^{-3}$ ) is fast enough to maintain hot, but thermalized distributions. The results are plotted in Fig. 3: The sample with  $\tau = 1.5 \text{ ps}$  (full squares) shows a substantially slower cooling of the carrier distribution. This slower cooling can be understood through the ultrafast trapping and recombination that occurs preferentially near the band gap.<sup>16</sup> The loss of carriers with low energy leads to a decrease of the total energy-loss rate, which is known as "recombination heating."<sup>20</sup> The higher temperature at later times, as compared to the lattice temperature, is due to the generation of hot phonons.

The theoretical curves in Fig. 3 are the results of ensemble MC calculations, taking into account the same energy dependence of the trapping and recombination as in the simulation of the inverted luminescence spectra. Also, the calculation shows a slower cooling of the sample with short carrier lifetime. The inset in Fig. 3 shows the difference of the cooling curves both for experiment and theory, with good agreement for the chosen value of the parameter  $K$  (energy dependence of the recombination). We conclude that the same energy dependence of the trapping rate—higher rate at low carrier energies—is present in the sample with  $\tau = 95 \text{ fs}$ . This clearly works against the thermalization and energy relaxation processes, and enhances the intraband inversion. We

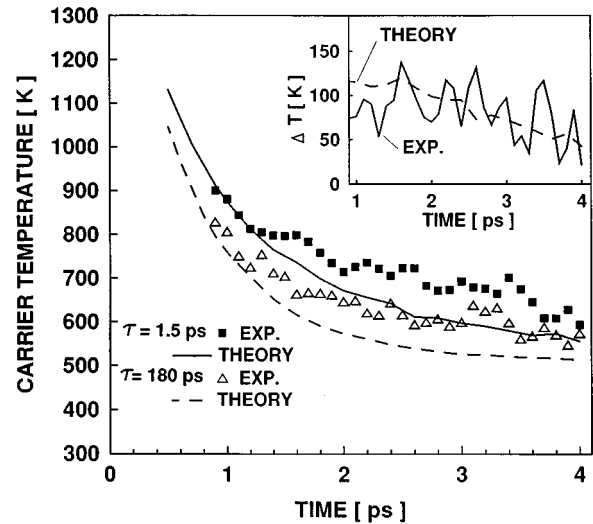


FIG. 3. Carrier temperatures as a function of time, observed in the time-resolved luminescence spectra, for two samples with different proton-bombardment doses, resulting in lifetimes of 1.5 ps (full squares) and 180 ps (triangles). Lines: Theoretical Monte Carlo simulations. Inset: Temperature difference of the two samples, as a function of time.

want to mention at this point, that hot phonons generated by the trapping and nonradiative recombination<sup>21</sup> generally would produce a similar effect. The generation of hot phonons, however, has to be considered only at high carrier concentrations. The intraband inversion in the sample with  $\tau = 95 \text{ fs}$  has been observed at low carrier densities ( $n \sim 3 \times 10^{16} \text{ cm}^{-3}$ ), where hot phonon effects play a minor role. We want to emphasize at this point, that hot phonons are generated also by nonradiative recombination and, therefore, will contribute to the relaxation processes at lower excitation than in undamaged material.

The realization of inversion within a continuous band of a semiconductor has interesting consequences for the research on stimulated emission within one energy band of a semiconductor.<sup>3</sup> Intraband inversion is the first condition for the solid-state analog of the free-electron laser,<sup>22</sup> where the stimulated radiative transitions within a continuous band are used. The demonstration of intraband inversion averaged over the complete lifetime of electron-hole pairs in the bands indicates that, in principle, the inversion can be maintained also in steady state, using continuous-wave excitation. The use of intraband radiative transitions, such as free-carrier emission through momentum scattering processes<sup>23</sup> or grating structures for the momentum conservation,<sup>24</sup> together with thicker samples necessary for a mid- and far-infrared waveguiding, should make such devices possible in the future. Major questions, however, are still open at this point, such as the absorption into higher band states, as well as additional radiative processes, due to the trap states and recombination centers.

In conclusion, we have proven that the time-integrated carrier distributions of photoexcited electrons and holes can be inverted in semiconductors with ultrashort carrier lifetimes.<sup>25</sup> Carrier trapping and recombination in the time range of 100 fs lead to strongly inverted luminescence spec-

tra at carrier densities well below  $10^{17} \text{ cm}^{-3}$ . At these concentrations, the thermalization process is slow enough ( $\sim 100$  fs), so that the initially injected carrier distributions still dominate the time-averaged energy distributions. Applications for stimulated intraband optical transitions are promising.

We acknowledge the contributions of L. Palmetshofer, Linz, who performed the proton bombardment. This work has been supported by the Jubiläumsfond der Österreichischen Nationalbank (ÖNB) under Project No. 5059, and by the Fonds zur Förderung der Wissenschaftlichen Forschung (FWF) under Project No. 10065.

- 
- <sup>1</sup>For a review, see, e.g., *Hot Carriers in Semiconductor Nanostructures*, edited by J. Shah (Academic, New York, 1992).
- <sup>2</sup>A. Leitensdorfer *et al.*, Phys. Rev. Lett. **73**, 1687 (1994).
- <sup>3</sup>K. Unterrainer, C. Kremser, E. Gornik, C. R. Pidgeon, Yu. L. Ivanov, and E. E. Haller, Phys. Rev. Lett. **64**, 2277 (1990); J. Faist *et al.*, Science **264**, 553 (1994).
- <sup>4</sup>C. V. Shank, R. L. Fork, R. F. Leheny, and J. Shah, Phys. Rev. Lett. **42**, 112 (1979).
- <sup>5</sup>J. L. Oudar *et al.*, Phys. Rev. Lett. **55**, 2074 (1985).
- <sup>6</sup>W. H. Knox, D. S. Chemla, G. Livescu, J. E. Cunningham, and J. H. Henry, Phys. Rev. Lett. **61**, 1290 (1988).
- <sup>7</sup>T. Gong, P. M. Fauchet, J. F. Young, and P. J. Kelly, Phys. Rev. B **44**, 6542 (1991).
- <sup>8</sup>U. Hohenester, P. Supancic, P. Kocevar, X. Q. Zhou, W. Kütt, and H. Kurz, Phys. Rev. B **47**, 13 233 (1993).
- <sup>9</sup>L. Rota, P. Lugli, T. Elsässer, and J. Shah, Phys. Rev. B **47**, 4226 (1993).
- <sup>10</sup>D. W. Snoke, W. W. Rühle, Y.-C. Lu, and E. Bauser, Phys. Rev. Lett. **68**, 990 (1992).
- <sup>11</sup>J. A. Kash, Phys. Rev. B **40**, 3455 (1989); G. Fasol, W. Hackenberg, H. P. Hughes, K. Ploog, E. Bauser, and H. Kano, *ibid.* **41**, 1461 (1990); J. Kash, *ibid.* **48**, 18 336 (1993).
- <sup>12</sup>S. Hunsche, H. Heesel, A. Ewertz, H. Kurz, and J. H. Collet, Phys. Rev. B **48**, 17 818 (1993).
- <sup>13</sup>M. Combescot, Solid State Commun. **62**, 587 (1987).
- <sup>14</sup>R. A. Höpfel, Solid-State Electron. **QE-32**, 1781 (1989).
- <sup>15</sup>K. Lamprecht, S. Juen, L. Palmetshofer, and R. A. Höpfel, Appl. Phys. Lett. **59**, 926 (1991).
- <sup>16</sup>For a review on trapping and recombination centers, see, e.g., *Deep Centers in Semiconductors*, edited by S. Pantelides (Gordon and Breach, New York, 1992).
- <sup>17</sup>P. R. Smith, D. H. Auston, A. M. Johnson, and W. M. Augustyniak, Appl. Phys. Lett. **38**, 47 (1981).
- <sup>18</sup>J. Shah, IEEE J. Quantum Electron. **24**, 276 (1988).
- <sup>19</sup>H. B. Bebb and E. W. Williams, in *Transport and Optical Phenomena*, edited by H. Hovel, Semiconductors and Semimetals Vol. 8 (Academic, New York, 1972), Chap. 4. Coherent effects can be neglected, since the phase relaxation time of photoexcited free carriers is of the order of 10 fs.
- <sup>20</sup>D. Bimberg and J. Mycielski, Phys. Rev. B **31**, 5490 (1985).
- <sup>21</sup>X. Q. Zhou, H. M. van Driel, W. W. Rühle, and K. Ploog, Phys. Rev. B **46**, 16 148 (1992).
- <sup>22</sup>IEEE J. Quantum Electron. **QE-27**, 2506 (1991), special issue on free-electron lasers.
- <sup>23</sup>R. A. Höpfel and G. Weimann, Appl. Phys. Lett. **46**, 291 (1985).
- <sup>24</sup>E. Gornik, R. Christanell, R. Lassnig, W. Beinstingl, K. Berthold, and G. Weimann, Solid-State Electron. **31**, 751 (1988).
- <sup>25</sup>A. Krotkus, S. Marcinkevicius, and R. Viselga (unpublished).